JACS
JOURNAL OF THE AMERICAN CHEMICAL SOCIETY
Article
pubs.acs.org/JACS

Different Reactivity of the Various Platinum Oxides and Chemisorbed Oxygen in CO Oxidation on Pt(111)

Daniel Miller,[†] Hernan Sanchez Casalongue,[†] Hendrik Bluhm,[‡] Hirohito Ogasawara,[†,§] Anders Nilsson,[†,§] and Sarp Kaya*[,†,∥]

[†]SUNCAT Center for Interface Science and Catalysis and [§]Stanford Synchrotron Radiation Lightsource, SLAC National Accelerator Laboratory, 2575 Sand Hill Rd, Menlo Park, California 94025, United States

[‡]Chemical Sciences Division, Lawrence Berkeley National Lab, Berkeley, California 94720, United States

[∥]Department of Chemistry, Koc University, Rumelifeneri Yolu, Sariyer, 34450, Istanbul Turkey

ABSTRACT: We have used X-ray photoelectron spectroscopy and polarization-resolved O *K*-edge X-ray absorption spectroscopy to investigate the reactivity of various oxygen covered Pt(111) surfaces, which emerge under high temperature and pressure conditions, toward CO. We find that the reactivity of the O/Pt(111) system decreases monotonically with increasing oxygen coverage. Of the three surface oxygen phases, viz., chemisorbed oxygen (O_{ad}), a PtO-like surface oxide, and α-PtO_2 trilayers, O_{ad} exhibits the highest reactivity toward CO, whereas α-PtO_2 trilayers exhibit the lowest. Pt(111) surfaces fully terminated by α-PtO_2 trilayers are inert to CO. Here it is proposed that the reactive phase is either O_{ad} or PtO-like surface oxide phase on bare non-CO poisoned Pt regions with PtO_2 as majority spectator species.

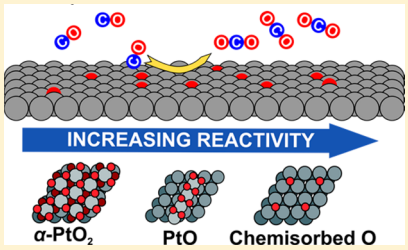

1. INTRODUCTION

Owing to the widespread use of Pt as oxidation catalyst in catalytic converters and in polymer-electrolyte-membrane fuel cells (PEMFCs), CO oxidation over well-defined Pt single-crystal surfaces has been closely studied under conditions ranging from vacuum to ambient pressure.[1−4] Despite intense scrutiny, it remains unclear which oxygen species on Pt surfaces are more or less reactive for CO oxidation.

CO oxidation in ultra-high-vacuum (UHV; $P < 1 \times 10^{-5}$ Torr) conditions proceeds via a Langmuir−Hinshelwood (LH) mechanism in which the active oxygen phase is chemisorbed oxygen (O_{ad}).[1,2,5,6] The barrier (E_a) to this LH process depends sensitively on the relative morphology of O_{ad} and adsorbed CO (CO_{ad}): on both Pt(110) and Pt(111), the observed reaction order in O_{ad} below the CO_{ad} desorption onset ($T \sim 400$ K) is ~0.5, which suggests that CO_2 formation on those surfaces is confined to the boundaries of chemisorbed O_{ad} domains.[1,2,6] The active oxygen phase during catalysis at realistic conditions, in contrast, has not been established, because techniques that probe surface speciation, e.g., X-ray photoelectron spectroscopy (XPS), are typically incompatible with industrially relevant pressure and temperature conditions ($P \sim 1$ bar, $T > 300$ K). Furthermore, most techniques that can interrogate some property of a Pt surface *in situ* under realistic conditions, e.g., high-temperature scanning tunneling microscopy (STM), X-ray absorption near-edge structure (XANES), and surface X-ray diffraction (SXRD), lack the sensitivity needed to detect minority surface species. Consequently, the oxygen phases identified as active by previous *in situ* studies could in principle be majority spectator species. There is considerable debate, for example, as to whether the high activity of Pt surfaces under nonstoichiometric, oxidizing conditions [i.e., under conditions where $P(O_2)/P(CO) > 1/2$] arises from the atomically thin surface oxide observed in most *in situ* studies or from a minority chemisorbed species that has to date eluded detection.[7−12]

Significantly, not only is the active phase under industrially relevant conditions controversial, it is also unclear which surface-oxygen phase of Pt is most reactive toward CO. Indeed, previous studies reach contradictory conclusions regarding the relative activities of O_{ad} and surface-oxide (PtO_x) phases. Isothermal rate measurements of PtO_x/Pt(111) and O_{ad}/Pt(111) films by Weaver et al. indicate that the rate of CO oxidation diminishes monotonically as the oxygen coverage [$\Theta(O)$; henceforth, $\Theta(O)$ will denote the coverage of surface-oxygen species exclusive of CO_{ad}, i.e., $\Theta(O) = \Theta(O_{tot}) - \Theta(CO_{ad})$] increases, which implies that PtO_x phases are less active than chemisorbed oxygen.[13] Conversely, titration studies of oxygen-precovered Pt(332)[14] and Pt(110)−(1 × 2)[15] surfaces suggest that Pt surface oxides could be more active toward CO: for Pt(332), a one-dimensional (1-D) step-edge surface oxide has been reported to disappear more readily than O_{ad} on the terraces,[14,16] while for Pt(110) it has been proposed that the α-PtO_2 phase and chemisorbed (12 × 2)−2O_{ad} domains react comparably fast.[15] These results are difficult to reconcile with the conclusion of Weaver et al.[11] that oxide phases inhibit CO oxidation on Pt(111), for two reasons: first, the step-edge oxide on Pt(332) exhibits the same square-planar Pt coordination and striped, 1-D morphology as the PtO-like surface oxide that forms on Pt(111);[17] and second, α-PtO_2 trilayers are precursors to bulk-oxide growth on both Pt(110)−(1 × 2)[7,18] and Pt(111).[11,17]

Received: December 25, 2013
Published: April 7, 2014

   dx.doi.org/10.1021/ja413125q | *J. Am. Chem. Soc.* 2014, 136, 6340−6347

This work aims to establish the relative activities for CO oxidation of the O_{ad} and PtO_x phases on Pt(111). Using a photoemission system that can operate at near-ambient pressures (P < 10 Torr),[19] we have followed the titration of oxygen-precovered Pt(111) surfaces with CO by means of X-ray absorption spectroscopy (XAS) and XPS. Unambiguous signatures of oxygen speciation[17] from O *K*-edge XAS and Pt 4f XPS allow us to compare directly the relative activities of the three surface-oxygen phases that can be generated by exposing Pt(111) to O_2 above 300 K: O_{ad}, PtO-like stripes (alternately denoted "4O"), and α-PtO_2 trilayers. We find that surface oxides react with CO more slowly than do O_{ad} domains. Crucially, α-PtO_2 trilayers are dramatically less active than either the chemisorbed or 4O phases: at 300 K, CO neither adsorbs on nor reacts with Pt(111) surfaces fully terminated by α-PtO_2 trilayers [$\Theta(O) \geq 1.6$ ML]. Based on the order of activity established in the present article, we conclude that the correlation between surface oxidation and increased activity observed in previous *in situ* studies does not prove that PtO_x phases are intrinsically more reactive than O_{ad} domains, as has been widely proposed. Rather, this correlation confirms only that CO_{ad}-saturated Pt(111) surfaces inhibit O_2 dissociation and are therefore drastically less reactive than surfaces covered by either O_{ad} or PtO_x phases. Our data and those of previous authors can be reconciled if we assume that under oxygen-rich conditions, it is possible to generate regions of bare Pt not poisoned by CO within which O_{ad} or PtO-like stripes are the active species for CO oxidation. Regions of PtO_2 can coexist with the active O_{ad} and PtO-like stripes under oxygen-rich conditions, but as a majority spectator species, rather than as an active phase.

2. METHODS

The experiments were performed at the variable phase undulator beamline 11.0.2 of the Advanced Light Source (ALS) using a chamber equipped to perform photoemission spectroscopy at pressures of up to 10 Torr.[19] The base pressure for all titration measurements was better than 1×10^{-9} Torr.

A Pt(111) disk (Ø10 mm × 2 mm thick) was cleaned by successive sputter–anneal cycles (annealing temperature = 1100 K) and cooling in oxygen [$P(O_2) = 1 \times 10^{-6}$ Torr; T = 800–400 K]. Oxygen-precovered surfaces were prepared by dosing up to 10 Torr O_2 between 300 and 800 K. $\Theta(O)$ for each sample was determined by comparing the ratio of the integrated intensities of the Pt 4p and O 1s XPS peaks, I(Pt 4p)/I(O 1s), against the corresponding ratio for a saturated $p(2 \times 2)$–O_{ad} adlayer, which has an oxygen coverage of 0.25 ML.[20−22]

The CO oxidation activity of oxygen layers were titrated by backfilling the chamber with a constant pressure of CO [$1 \times 10^{-8} < P(CO) < 1 \times 10^{-5}$]. To eliminate contamination from Ni carbonyls, the CO was passed over a trap consisting of heated Cu gauze (~250 °C) and supplied to the chamber using Cu tubing; we could not discern any traces of Ni on the surface using Ni 3p XPS.

In both the XPS and XAS measurements, the sample was illuminated at grazing incidence such that the angle (ϕ) between the sample surface and the propagation direction of the incoming beam was ~10°; the electron-emission angle in this geometry was ~35°. Unless otherwise specified, all XP and XA spectra were acquired *ex situ*, i.e., after evacuating CO and at base pressure.

The binding energies (BE) of all XP spectra are referenced to the Fermi level (E_F) of Pt. From the full-width at half-maximum of the Fermi edge, we estimate that the resolution of all XPS measurements presented here is better than 0.3 eV. Unless otherwise specified, O 1s and Pt 4f XPS were recorded using incident photon energies ($\hbar\omega$) of 735 and 275 eV, respectively. A Shirley-type background has been subtracted from all XP spectra. All of the Pt 4f spectra shown in the present article are normalized to the height of either the bulk Pt $4f_{5/2}$ peak at 74.3 eV or the bulk Pt $4f_{7/2}$ peak at 70.9 eV; the O 1s XP spectra are not normalized.

O *K*-edge XAS was recorded using an electron spectrometer by monitoring the yield of O(*KLL*) Auger electrons while sweeping $\hbar\omega$ from 525 to 555 eV; the overall resolution of these measurements is better than 0.1 eV. By changing the phase of the undulator, the **E**-vector of the linearly polarized incident beam could be oriented either parallel (ϕ = 0) or perpendicular ($\phi \sim 80°$) to the sample plane; the spectra thus recorded will henceforth be denoted in plane and out of plane, respectively. All spectra shown here reflect removal of the background contribution of the Pt substrate and are area normalized 30 eV above the O *K*-edge absorption threshold, i.e., at 550 eV.

3. RESULTS

3.1. Reactivity of α-PtO_2/Pt(111) toward CO. In order to examine the reactivity toward CO of α-PtO_2 trilayers, we exposed a Pt(111) crystal to 10 Torr O_2 for 10 min while repeatedly (~4 times) cycling its temperature between 300 and 800 K. O *K*-edge XAS (Figure 1a) and Pt 4f XPS (Figure 1b)

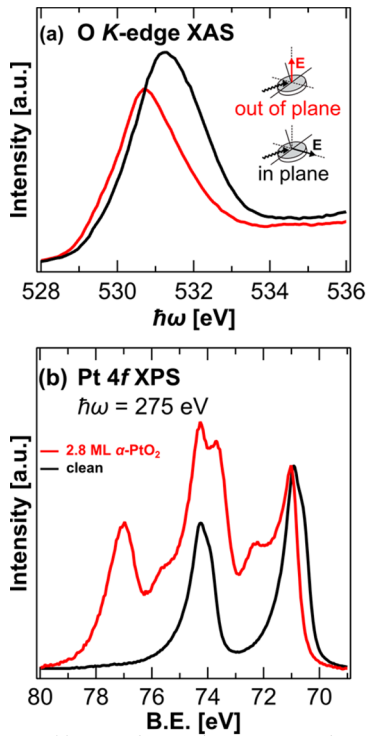

Figure 1. (a) In-plane (black line) and out-of-plane (red line) O *K*-edge XA spectra of a 2.8 ML α-PtO_2 film. (b) Pt 4f XP spectra of a 2.8 ML α-PtO_2 film (red line) and of an adsorbate-free Pt(111) surface (black line).

together with coverage estimates from O 1s XPS (Figure 2b) confirm that the surface thus prepared is fully covered by an α-PtO_2 film. O *K*-edge XA spectra exhibit a single feature centered at 530.8 and 531.2 eV in the out-of-plane and in-plane polarizations, respectively, which establishes that the oxygen layer is composed exclusively of α-PtO_2 trilayers.[17] Pt $4f_{5/2}$ XPS shows not only that oxide comprises α-PtO_2 trilayers but also that the underlying metallic substrate is fully covered: whereas Pt $4f_{7/2}$ features associated with bulk Pt (70.9 eV) and the α-PtO_2-like surface oxide (72.2 and 73.6 eV) are clearly resolved, there are no signatures of either adsorbate-free (70.5 eV) or O_{ad}-binding (71.1 eV) metallic surface sites. This is also seen as a lack of the low-energy resonance in the in-plane spectra

dx.doi.org/10.1021/ja413125q | J. Am. Chem. Soc. 2014, 136, 6340−6347

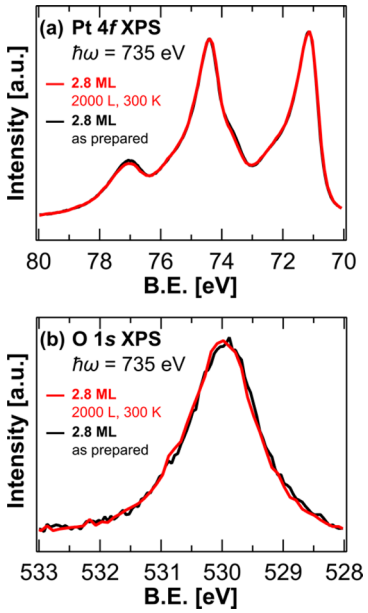

Figure 2. (a) Pt 4f and (b) O 1s XP spectra of an 2.8 α-PtO_2 film before (black lines) and after (red lines) exposure to 2000 L CO [$P(CO) = 1 \times 10^{-5}$ Torr] at 300 K.

related to O_{ad}.[17] The oxygen coverage of 2.8 ML, determined using O 1s XPS, is also consistent with the presence of multiple α-PtO_2 trilayers: based on the mismatch between the in-plane lattice constants of α- PtO_2 (3.10 Å) and Pt(111) (2.77 Å), we estimate that the α-PtO_2 film comprises ~1.8 trilayers {trilayers ~$2.8/[2 \times (2.77/3.10)^2] = 1.8$}. Given that the (1010) facet is the only stable low-index surface orthogonal to the (0001) surface,[23] we postulate that the α-PtO_2 film comprises α-PtO_2(0001) islands with (1010)-oriented edges.

The reactivity toward CO oxidation was examined by heating the oxide film in CO. While the 2.8 ML oxide layer is inert to CO at 300 K, heating beyond ~350 K in the presence of 1×10^{-5} Torr CO triggered the removal of oxygen. Figure 2(a) shows that the 2.8 ML oxide layer is unchanged by exposure to 2000 L CO [$P(CO) = 1 \times 10^{-5}$ Torr] at 300 K. In particular, O 1s (Figure 2b) and Pt 4f XP (Figure 2a) spectra indicate that $\Theta(O)$ remains constant and that CO does not adsorb. This accords with the observation of Weaver et al. that a 1.7 ML α-PtO_2/Pt(111) film reacted with CO when $T \geq 400$ K, albeit after a long induction period.

We do not observe that CO reduces the α-PtO_2-like surface oxide to other oxygen phases, e.g., chemisorbed oxygen, during CO oxidation. Instead, we observe that a CO-covered metallic surface is generated. Specifically, the only readily discernible change in Pt $4f_{5/2}$ XPS (Figure 3a) is a steady attenuation of features at 75.6 and 77.0 eV associated with the α-PtO_2 phase. We note that the presence of CO_{ad} cannot be readily resolved using Pt 4f XPS, because features from on-top (75.4 eV) and bridge (74.8 eV) CO_{ad} overlap with the 75.6 eV α-PtO_2 feature.[20] O *K*-edge XAS, however, confirms that both α-PtO_2 trilayers and CO_{ad} remain on the surface after partially reducing the 2.8 ML oxide layer: in the representative out-of-plane spectrum shown in Figure 3b, the peaks at 531.2 and 533.1 eV can be respectively assigned to α-PtO_2 and the π^* resonance of CO. Removing the residual CO_{ad} by flashing to 450 K generates a CO_{ad}-free, partial oxide film [$\Theta(O) = 0.46$ ML] with XA spectra nearly identical to those of the intact 2.8 ML oxide layer (Figure 3c). The coordination environment of

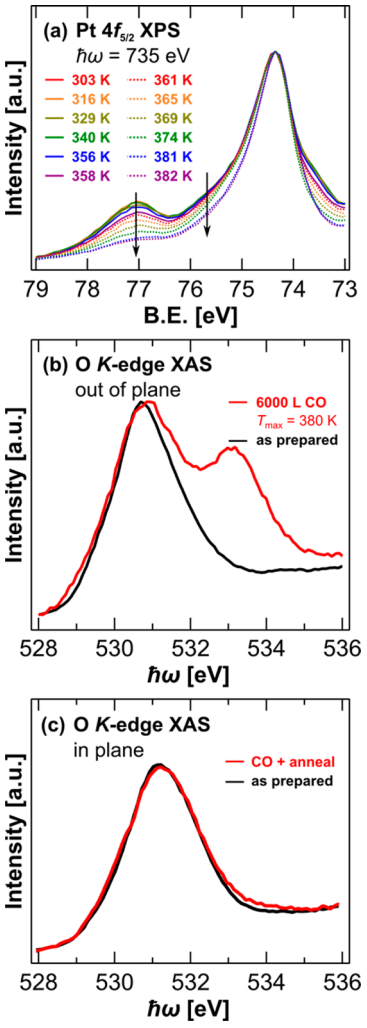

Figure 3. (a) Pt $4f_{5/2}$ XP spectra recorded *in situ* while heating a 2.8 ML α-PtO_2 film from 300 to 380 K in the presence of 1×10^{-5} Torr CO. (b) Out-of-plane O *K*-edge XA spectra before (black line) and after (red line) the 6000 L CO dose. Subsequent annealing to ~450 K removed CO_{ad}, yielding the in-plane O *K*-edge XA spectrum shown by the red line in (c).

most of the Pt atoms within the α-PtO_2 film is thus unchanged following reaction with CO; Weaver et al. reached similar conclusions from temperature-programmed desorption (TPD) studies of partially reduced α-PtO_2/Pt(111) films.

3.2. Relative Reactivities of α-PtO_2 Trilayers and Chemisorbed Oxygen. We compared the reactivities of α-PtO_2 trilayers and chemisorbed oxygen using an oxygen layer comprising both phases.

The sample was prepared via a two-step procedure. First, we generated a Pt surface sparsely covered by α-PtO_2 islands [$\Theta(O) = 0.27$ ML] by reacting a α-PtO_2 film with CO at 400 K and subsequently flashing to 450 K to desorb residual CO_{ad}. Second, the surface was exposed to 1×10^{-4} Torr O_2 at 300 K for 15 min, yielding a mixed O_{ad}/α-PtO_2 layer with a total oxygen coverage of 0.47 ML.

Both Pt $4f_{5/2}$ XPS (Figure 4a) and O *K*-edge XAS (Figure 4b) confirm that the 0.47 ML mixed oxygen layer comprises α-PtO_2 islands surrounded by $p(2 \times 2)$–O_{ad} domains. The Pt $4f_{5/2}$ XP spectrum of the 0.27 ML α-PtO_2 film exhibits clear signatures of adsorbate-free surface Pt sites (73.8 eV) and α-PtO_2 trilayers (75.6 and 77.0 eV), while the spectrum of the

dx.doi.org/10.1021/ja413125q | J. Am. Chem. Soc. 2014, 136, 6340–6347

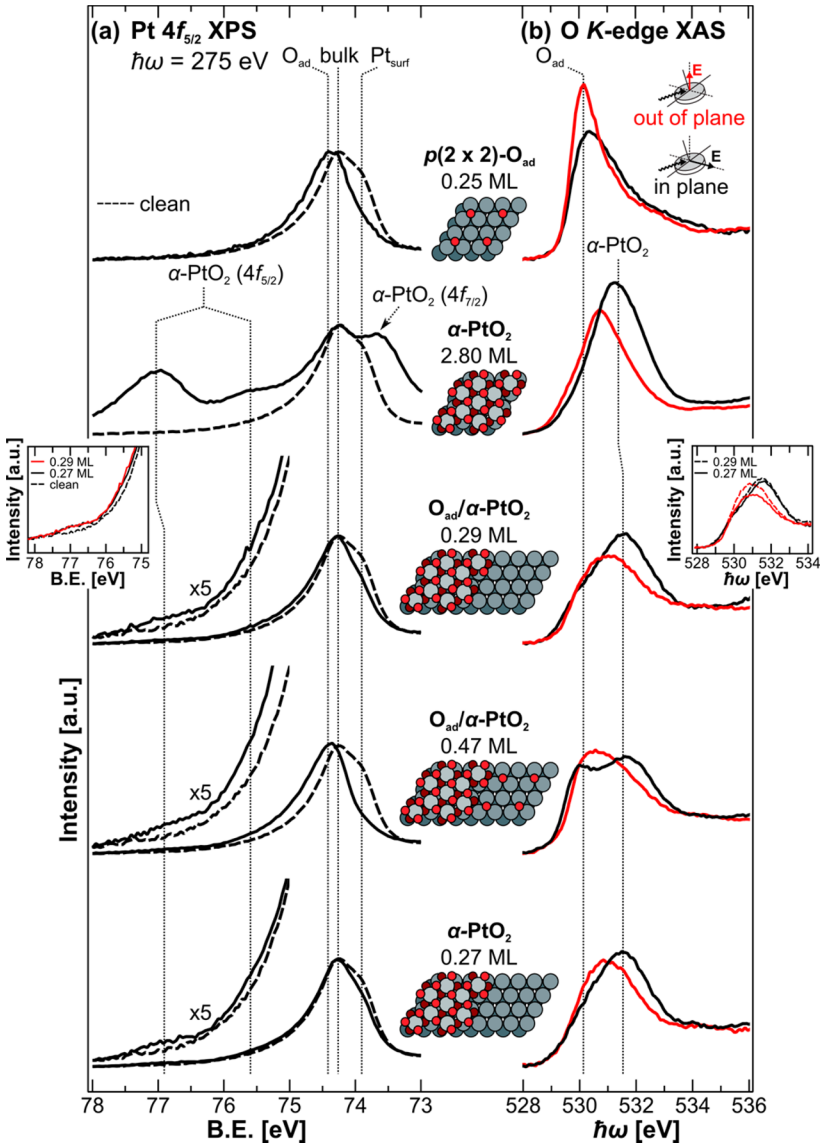

Figure 4. (a) Pt $4f_{5/2}$ XP and (b) O *K*-edge XA spectra of (in order from bottom to top) a 0.27 ML α-PtO_2 film; a 0.47 ML mixed O_{ad}/α-PtO_2 film generated by exposing the 0.27 ML film to 1×10^{-4} Torr O_2; a 0.29 ML O_{ad}/α-PtO_2 film generated by exposing the 0.47 ML mixed film to 1 L CO; a 2.8 ML α-PtO_2 film; a saturated $p(2 \times 2)$−O_{ad} adlayer. Each spectrum in (a) is compared against the spectrum of an adsorbate-free Pt(111) surface (dashed lines). Red and black traces in (b) are out-of-plane and in-plane polarized, respectively. Schematic structure models are shown at the center of the figure. The insets directly overlay the Pt $4f_{5/2}$ XP (left inset) and O *K*-edge XA (right inset) spectra of the as-prepared 0.27 ML and CO-exposed 0.29 ML films.

0.47 ML mixed film shows an additional feature at 74.6 eV arising from Pt atoms bound to O_{ad}. The conclusions from O *K*-edge XAS are analogous: in addition to an oxide-derived resonance, the mixed 0.47 ML layer exhibits a near-edge resonance at 529.9 eV attributable to chemisorbed O_{ad}. By deconvoluting the Pt 4f XP spectra of the 0.27 and 0.47 ML films, we ascertain that dosing O_2 reduces the coverage of adsorbate-free Pt surface sites (henceforth denoted Pt_{surf} sites) by ∼0.70 ML. This corroborates that exposure to oxygen covers all initially available Pt_{surf} sites with $p(2 \times 2)$−O_{ad} domains: assuming ∼0.70 ML surface Pt sites are bound to O_{ad} in $p(2 \times 2)$−O_{ad} domains, we estimate that the coverage of O_{ad} is ∼0.23 ML [$\Theta(O_{ad}) \sim 0.70/3 = 0.23$ ML], which agrees with the ∼0.20 ML increase in coverage observed after dosing O_2 [$\Theta(O_{ad}) \sim 0.47-0.27$ ML = 0.20 ML].

Exposing the mixed phase to 1 L CO [$P(CO) = 1 \times 10^{-8}$ Torr] removes only the $p(2 \times 2)$−O_{ad} domains. Whereas the Pt $4f_{5/2}$ peaks associated with α-PtO_2 islands are unchanged after dosing CO (inset, Figure 4a), the intensity of the chemisorbed feature is drastically reduced. Moreover, the intensity lost from the chemisorbed Pt $4f_{5/2}$ feature nearly matches that recovered by the surface peak, which further supports the claim that only the O_{ad} domains react. O *K*-edge XAS also shows that the oxygen species that persist after titration are composed principally of α-PtO_2 islands, since chemisorbed O_{ad} manifests as a strong peak broadening at the low-energy side of the α-PtO_2 resonance (inset, Figure 4b). Since CO_{ad} was not detected while dosing CO using either O 1s or C 1s XPS, the reaction rate must be limited by the incoming CO flux at the pressure we employed (1×10^{-8} Torr). This accords with our claim that only chemisorbed oxygen reacted, since it is known that, at 295 K, CO impingement limits the reaction rate when $P(CO) < 5 \times 10^{-7}$ Torr.[1,6]

dx.doi.org/10.1021/ja413125q | J. Am. Chem. Soc. 2014, 136, 6340−6347

3.3. Relative Reactivities of α-PtO_2 Trilayers and PtO-Like Stripes. We used a surface oxygen layer composed of a mixture of the 4O and α-PtO_2-like surface oxides [$\Theta(O)$ = 1.1 ML] to evaluate the reactivity of PtO-like and α-PtO_2-like surface oxides.

The sample was prepared by heating Pt(111) in 0.5 Torr O_2 at 620 K. Pt 4f XPS (Figure 5a), O 1s XPS (Figure 5b) and O

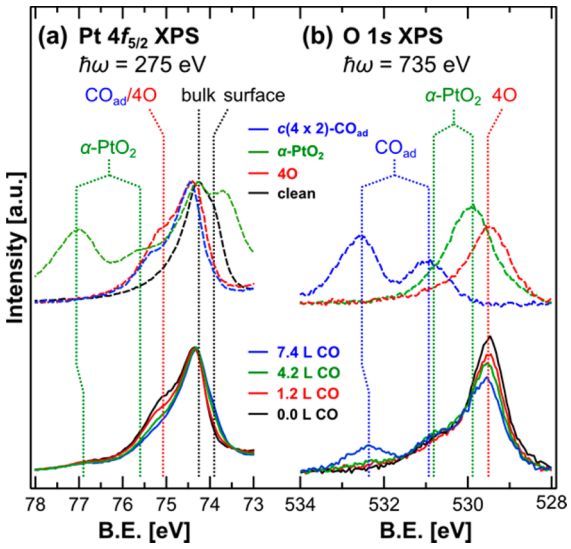

Figure 5. (a) (solid lines at bottom) Pt $4f_{5/2}$ XP spectra of a mixed PtO/α-PtO_2 film after exposure to 0.0 L (black), 1.2 L (red), 4.2 L (green), and 7.4 L (blue) CO; (dashed lines at top) reference Pt $4f_{5/2}$ XP spectra of an adsorbate-free Pt(111) surface (black), a 1.1 ML 4O film (red), a 2.8 ML α-PtO_2 film (green), and a 0.5 ML $c(4 \times 2)$–$2CO_{ad}$ adlayer (blue). The corresponding O 1s XP spectra are shown in (b).

K-edge XAS (Figure 6) show clear signatures of the two phases: The Pt $4f_{5/2}$ XP spectrum exhibits a pronounced peak characteristic of α-PtO_2 trilayers at 77.0 eV as well as a broad shoulder centered at 75.1 eV that, based on the measurements of pure PtO_x/Pt(111) phases outlined in Miller et al.,[17] subsumes components at 75.0 and 75.3 eV associated with the 4O and α-PtO_2-like surface oxides, respectively. Since the feature at 77.0 eV is considerably weaker than the shoulder at 75.1 eV, the intensity of the shoulder must derive principally from the 4O component. Indeed, the O *K*-edge XA spectra (Figure 6) of the mixed 1.1 ML layer deviate only slightly from those of a pure "4O" phase. Neglecting the minor contribution of the α-PtO_2 component to the shoulder at ~75.1 eV, we obtain an upper bound of 0.78 ML for the fraction of surface Pt atoms within the PtO-like surface oxide; the remaining 0.22 ML must be incorporated within α-PtO_2 trilayers, because we cannot discern a Pt $4f_{5/2}$ component at 73.8 eV ascribable to Pt_{surf} sites. From this information, we estimate that $\Theta(O) \sim 1.2$ ML [$\Theta(O) \sim 0.78 \times 1 + 0.22 \times 2$ ML = 1.2 ML], which agrees with the coverage of 1.1 ML determined from O 1s XPS.

When the 1.1 ML mixed layer is dosed with 1×10^{-8} Torr CO at 300 K, the PtO-like stripes disappear more rapidly than the α-PtO_2 islands. Indeed, aside from the growing feature at ~533.5 eV, which is due to transitions to the π^* resonance of CO_{ad}, the O *K*-edge XA spectra of the mixed PtO/α-PtO_2 layer steadily approach those of a pure α-PtO_2 film with increasing CO exposure. In particular, regardless of incident polarization, the near-threshold, PtO-derived feature (529.8 eV) attenuates

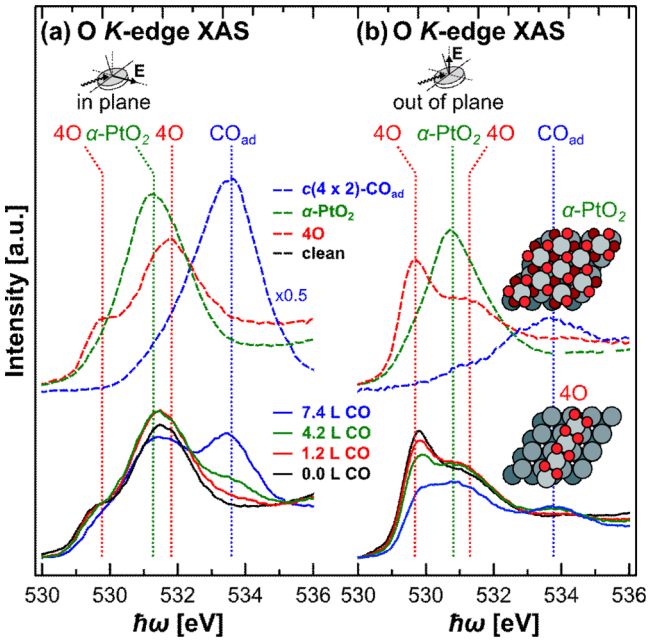

Figure 6. (a) (solid lines at bottom) In-plane O *K*-edge XA spectra of a mixed PtO/α-PtO_2 film before (black) and after exposure to 1.2 L (red), 4.2 L (green), and 7.4 L (blue) CO; (dashed lines at top) reference in-plane O *K*-edge XA spectra of a 1.1 ML 4O film (red), a 2.8 ML α-PtO_2 film (green), and a 0.5 ML $c(4 \times 2)$–$2CO_{ad}$ adlayer (blue). The corresponding out-of-plane O *K*-edge XA spectra are shown in (b). The ball models of the α-PtO_2 and 4O (PtO-like striped phase) structures were also presented.

more rapidly than does the higher-energy α-PtO_2-derived feature. Pt 4f XPS corroborates that dosing CO preferentially removes the PtO-like surface oxide: despite subsuming growing CO_{ad} components—bridge and on-top CO_{ad} within $c(4 \times 2)$–$2CO_{ad}$ domains yield features at 74.8 and 75.4 eV, respectively[20]—the shoulder at ~75.1 eV attenuates faster than the α-PtO_2 component at ~77.0 eV. The simultaneous intensity gain in Pt $4f_{5/2}$ surface component at 73.8 eV also suggests that adsorbate-free Pt(111) sites are generated.

Based on Pt 4f XPS and O *K*-edge XAS, the PtO-like stripes do not decompose to other surface-oxygen phases during CO oxidation. O *K*-edge XAS reveals that the intensity of the near-edge, PtO-derived feature at ~529.8 eV (Figure 4b) progressively decreases after each CO dose; the decomposition of the 4O phase to O_{ad} would produce the opposite effect, since the O_{ad} resonance appears at the same energy as the 4O resonance but exhibits weaker polarization dependence. In Pt $4f_{5/2}$ XPS, on the other hand, we cannot detect any feature at ~74.6 (i.e., on the high-energy-side of the bulk component) that would suggest O_{ad} formation. We therefore propose that both the PtO-like and α-PtO_2-like oxides react directly with CO, i.e., without prior decomposition.

3.4. Activity versus Total Oxygen Coverage. To establish how reactivity varies with $\Theta(O)$, we measured the rate at which surface-oxygen species are removed upon exposure to CO. Specifically, O 1s and Pt 4f XP spectra were recorded *in situ* while exposing oxygen-precovered Pt(111) surfaces to CO (Figure 7). We examined three systems: a 2.8 ML α-PtO_2 film (see Section 3.1); a mixture of $p(2 \times 2)$–O_{ad} and α-PtO_2 domains with an oxygen coverage of 0.47 ML (see Section 3.2); a mixture of PtO and α-PtO_2 with a total oxygen coverage of 1.4 ML (see Section 3.3). In addition, activity

dx.doi.org/10.1021/ja413125q | J. Am. Chem. Soc. 2014, 136, 6340–6347

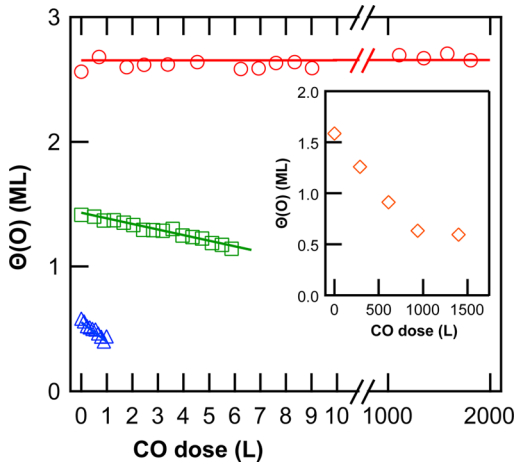

Figure 7. The coverage of surface-oxygen species [Θ(O)] while dosing CO, as determined using *in situ* O 1s XPS, for three oxygen layers on Pt(111): (red circles) an α-PtO_2 film with an initial coverage of 2.8 ML; (green squares) a 4O/α-PtO_2 mixture with an initial coverage of 1.4 ML; (blue triangles) an O_{ad}/α-PtO_2 mixture with an initial coverage of 0.47 ML. The solid lines are guides to the eye. P(CO) was 1×10^{-8} Torr in all measurements except that of the 2.8 ML α-PtO_2 film, for which a pressure of 1×10^{-5} Torr was employed. Inset: CO dose-dependent change of the surface-oxygen species from α-PtO_2 partially covering the surface. Note that Θ(O) excludes the coverage of CO_{ad}, i.e., $\Theta(O) = \Theta(O_{total}) - \Theta(CO)$.

studies of the α-PtO_2 islands were also performed since it is important to confirm the low reactivity of the α-PtO_2 phase also under the non-CO-adsorption-limited conditions. The α-PtO_2 islands were prepared by exposing 2.8 ML α-PtO_2 CO at 400 K until 1.6 ML coverage is reached. Island formation was confirmed by XPS, the appearance of the Pt $4f_{7/2}$ surface component indicated the formation of adsorbate free Pt sites (not shown). The PtO/α-PtO_2 and O_{ad}/α-PtO_2 mixtures were dosed with 1×10^{-8} Torr CO, while the pure α-PtO_2 film and islands were dosed with 1×10^{-5} Torr CO on account of their drastically lower reactivity; the substrate temperature in the measurements was 300 K except for α-PtO_2 islands (345−350 K).

Of the three oxygen layers we prepared, the α-PtO_2 film is clearly the least active for CO oxidation, despite the significantly higher CO flux employed. The activity of α-PtO_2 islands is also poor, as seen in the inset of Figure 7, the amount of CO dose required to reduce the islands is dramatically higher. The α-PtO_2 phase mixed with O_{ad} and 4O phases and α-PtO_2 islands coexisting with bare Pt surface sites remain intact at 300 K. As outlined in Section 3.2, only the $p(2 \times 2)$−O_{ad} domains react when the 0.47 ML O_{ad}/α-PtO_2 mixture is exposed to 1 L CO. The initial rate at which the 0.47 ML mixture is removed is therefore governed exclusively by the reactivity of chemisorbed oxygen. The partial-coverage data in Figure 7 clearly demonstrate that the chemisorbed domains in the 0.47 ML sample react more rapidly than do the two oxides (4O, α-PtO_2) comprising the 1.4 ML sample: at the same CO flux [P(CO) = 1×10^{-8} Torr], ∼1 L CO removes ∼0.2 ML chemisorbed oxygen, whereas ∼6 L is required to remove a similar amount of the PtO/α-PtO_2 mixture. The reactivity of oxygen-precovered Pt(111) surfaces for CO_{ad} oxidation thus decreases as the extent of surface oxidation increases. Specifically, chemisorbed domains exhibit the highest activity for CO oxidation, while α-PtO_2 trilayers exhibit the lowest activity.

4. DISCUSSION

Pt(111) surfaces fully terminated by α-PtO_2 films [Θ(O) ≥ 1.6 ML] and α-PtO_2 islands [Θ(O) ≤ 1.6 ML] are the least active of all the oxygen precovered surfaces considered in the study; they are inert to prolonged CO exposures (∼2000 L) below ∼350 K and react only slowly above that temperature. Our results also clearly demonstrate that the intrinsic reactivity toward CO of the O/Pt(111) system decreases monotonically with increasing surface oxidation, i.e., reactivity follows the sequence O_{ad} > 4O ≫ α-PtO_2. In this section, we seek both to account physically for this order of activity and to reconcile it with the ostensibly contradictory conclusions of prior *in situ* studies.

4.1. Mechanism of the Reactions of the O_{ad} and 4O Phases Mixed with α-PtO_2. On O_{ad}-precovered Pt(111) surfaces below the CO_{ad} desorption onset (i.e., T < 400 K), CO_2 formation occurs exclusively at the phase boundaries between $p(2 \times 2)$−O_{ad} and $c(4 \times 2)$−$2CO_{ad}$ domains.[16,24]

On Pt(111) surfaces partially terminated by α-PtO_2 trilayers, CO_{ad} oxidation is likely to proceed via an LH mechanism confined to coordinately unsaturated Pt and O surface sites (henceforth denoted Pt_{cus} and O_{cus} sites, respectively), e.g., (1010) facets at the boundaries of α-PtO_2(0001) domains and metal/α-PtO_2 phase boundaries. Since the majority of Pt_{cus} sites within the sparse 0.27 ML α-PtO_2 film must reside at metal/α-PtO_2 phase boundaries, the preferential removal of chemisorbed O_{ad} from the mixed O_{ad}/α-PtO_2 layer suggests that, on average, the edges of compact O_{ad} islands are more reactive than metal/α-PtO_2 phase boundaries. Although the sticking probability of CO at 300 K is dramatically lower on α-PtO_2(0001) surfaces than on O_{ad} domains (see Section 3.1), this effect alone cannot explain the lower activity of the α-PtO_2 islands, because at 300 K CO_{ad} molecules on bare metallic sites are highly mobile and can readily diffuse to the edges of α-PtO_2 islands. Indeed, the barrier to the diffusion of CO_{ad} [E_a(diff)] on Pt(111) terraces is reported to be ∼0.1 eV.[25]

Interestingly, density functional theory (DFT) simulations predict that the LH oxidation of CO_{ad} is more facile at favorably disposed $c(4 \times 2)$−$2CO_{ad}$/α-PtO_2 phase boundaries (E_a ∼ 0.08−0.24 eV) and at the (1010) facet of bulk α-PtO_2 (E_a ∼ 0.3 eV) than at the $c(4 \times 2)$−$2CO_{ad}$/$p(2 \times 2)$−O_{ad} phase boundary (E_a ∼ 0.5 eV).[16,24] If the barrier to removing defective α-PtO_2 trilayers were as low as ∼0.3 eV, however, the sparse α-PtO_2 islands would react instantaneously upon exposure to CO at room temperature. Since this is not observed, we speculate that the barrier to CO_{ad} oxidation at metal/α-PtO_2 boundaries must be much higher than the barrier at the edges of O_{ad} domains estimated from DFT as ∼0.5 eV.

Regarding the 4O/α-PtO_2 mixture, we note that the PtO-like surface oxide has a 1-D, striped morphology. Assuming that CO_{ad} oxidation follows a LH mechanism over both the 4O and α-PtO_2 phases but with very different rate constants, the following three factors could account for our observation that the 4O phase is more reactive: (1) the sticking probability of CO is higher on the 4O phase than on α-PtO_2(0001); (2) CO_{ad} oxidation is less activated over the 4O phase than at metal/α-PtO_2 phase boundaries; and (3) for a given oxygen coverage, the fraction of reactive oxygen sites is higher for the 4O phase. Of these three factors, only the first has been validated experimentally: the sticking coefficient of CO declines

dx.doi.org/10.1021/ja413125q | J. Am. Chem. Soc. 2014, 136, 6340−6347

monotonically with coverage, and at 100 K becomes immeasurably small once $\Theta(O)$ exceeds 1.5 ML.[11] Although sticking probability alone cannot fully rationalize the lower reactivity of the α-PtO_2 phase—CO should readily diffuse to the reactive boundaries of α-$PtO_2(0001)$ domains once Pt_{surf} sites become available—the relative contributions of the second and third factors outlined above cannot be specified based on our results. The DFT simulations of Petersen et al.,[23] however, support the hypothesis that the 4O phase is more reactive because of its higher fraction of active oxygen sites. The LH oxidation of CO_{ad} is predicted to encounter the same barrier ($E_a \sim 0.3$ eV) over both α-$PtO_2(1010)$ and (12×2)–$2O_{ad}$/Pt(100)–(2×1); the latter phase is structurally and morphologically analogous to the 4O surface oxide. However, whereas only the boundaries of α-PtO_2 islands are active for CO oxidation, Pedersen et al. predict that the adsorption and oxidation of CO_{ad} are weakly activated both within and at the boundaries of the (12×2)–$2O_{ad}$ phase. We note, however, that since E_a for the α-PtO_2 structure must be much higher than 0.5 eV (see Section 3.2), the 0.3 eV reaction barrier computed for the (12×2)–$2O_{ad}$ phase is an underestimate.

We conclude, therefore, that reaction occurs only with the O_{ad} and 4O phases under the present conditions. There is no indication that the α-PtO_2 islands react with chemisorbed CO following the removal of either O_{ad} or the 4O phase. We cannot exclude, however, that the PtO_2 phase does in fact react at its boundary, but with a rate constant that is orders of magnitude lower than that for the reaction of either O_{ad} or 4O with CO_{ad}.

4.2. Mechanism of the Reaction of α-PtO_2 with CO. CO is unlikely to adsorb on or react with defect-free α-$PtO_2(0001)$ surfaces, on account of the coordinative saturation of the surface Pt and O atoms. Consequently, CO_2 formation on Pt(111) surfaces fully terminated by α-PtO_2 [$\Theta(O) \geq 1.6$ ML], e.g., the 2.8 ML α-PtO_2 film considered in Section 3.1, which reacted only at elevated temperatures, must be confined to Pt_{cus} and O_{cus} sites.

A recent STM study of a Pt(111) surface oxidized using atomic O beams[13] reveals that the α-PtO_2-like surface oxide is not a continuous thin film but is instead arranged in a network of stripes aligned along the three high-symmetry axes of the Pt(111) substrate. For the 2.8 ML α-PtO_2 film, it is very likely that the stripes lack periodic superstructure, enclosing small α-$PtO_2(0001)$ domains with sizes that accord with previous estimates from SXRD (35–60 Å).[26,27] Moreover, since the (1010) facet is the only stable low-index surface orthogonal to the (0001) surface,[23] the stripes are likely to bounded by (1010)-oriented edges.

Indeed, DFT simulations performed by Pedersen et al. suggest that the active oxygen sites within α-PtO_2 films are located at the (1010)-oriented boundaries of α-$PtO_2(0001)$ domains: whereas on defect-free α-$PtO_2(0001)$ the barrier to CO adsorption is predicted to be prohibitively high [$E_a(\text{ads}) \sim 1.8$ eV], on the more open (1010) facet both adsorption [$E_a(\text{ads}) \sim 0.1$ eV] and CO_{ad} oxidation ($E_a \sim 0.3$ eV) are weakly activated.[23] Moreover, the same authors predict that the Eley–Rideal (ER) reaction of CO over α-$PtO_2(0001)$ is disfavored by ~1 eV with respect to the LH reaction of CO_{ad} over α-$PtO_2(1010)$. We therefore speculate that CO_2 formation on the 2.8 ML oxide film occurs exclusively at coordinately unsaturated Pt_{cus} sites, viz., the edges of and defects within α-$PtO_2(0001)$ islands. Similar reaction pathway holds true for PtO_2 islands coexisting with Pt sites available for CO adsorption (LH mechanism). The reactivity however depends on the availability of the Pt_{cus} sites at the boundaries of the α-PtO_2 islands. Obviously these are much less reactive than the O_{ad} or 4O phases.

4.3. Comparison with Prior Studies of CO Oxidation on Pt Surfaces. For vicinal Pt surfaces, e.g., Pt(332), it has been reported that 1-D step-edge oxides analogous to the PtO-like striped phase could be more active for CO oxidation than are chemisorbed oxygen atoms on the terraces.[14] Our experiments indicate that this is unlikely for the oxide that form on Pt(111). It has also been suggested based on oxidation experiments performed in mbar scale by Farkas et al. that the surface of Pt(111) might be covered with chemisorbed and oxide species.[27] In contrast to Farkas et al., we find that find chemisorbed oxygen phases are clearly the most active for CO oxidation; we emphasize, however, that our measurements were undertaken in a different pressure regime. The reactivity order we show with structural precision here is also consistent with the finding reported by the Weaver group,[11] which has also been stressed by the Goodman group.[28] Since the rate of loss of O_{ad} upon exposure to CO is greater than that of the 4O phase, our observations do not support the reaction scheme proposed for Pt(110) surface in similar environments.[15] Our results also indicate that the reaction takes place at the boundaries between different phases,[24] 4O and α-PtO_2 mixtures are consumed by CO reacting with under-coordinated oxygen atoms located near periphery.

5. CONCLUSIONS

Using XPS and polarization-resolved O K-edge XAS, we have investigated the reactivity toward CO of Pt(111) surfaces precovered with up to 2.8 ML of oxygen [$\Theta(O) \leq 2.8$ ML]. Our results indicate that the reactivity of the O/Pt(111) system decreases monotonically as the extent of surface oxidation increases: of the three surface oxygen phases that can be generated on Pt(111) by dosing O_2 above 300 K, viz., chemisorbed oxygen (O_{ad}), a PtO-like surface oxide, and α-PtO_2 trilayers, O_{ad} exhibits the highest reactivity toward CO, whereas α-PtO_2 trilayers exhibit the lowest. Significantly, we find that Pt(111) surfaces fully terminated by α-PtO_2 trilayers [$\Theta(O) \geq 1.6$ ML] are not active at all to CO oxidation when $T \leq 300$ K and $P(CO) \leq 1 \times 10^{-5}$ Torr.

The order of activity identified in the present study, $O_{ad} >$ 4O $\gg$ α-PtO_2 can be reconciled with prior *in situ* studies that report that incipient oxide growth coincides with increased CO_2 production, because in all such studies the onset of oxidation corresponds to a phase transition between a poisoned, CO_{ad}-saturated metallic surface and a more active, partially oxidized surface. Our results show that this active, partially oxidized surface must comprise regions of bare metallic Pt that coexist with O_{ad}- or 4O-covered regions. The dramatically lower intrinsic reactivity of the α-PtO_2-like surface oxide strongly suggests that the active phase for CO oxidation at high pressures is likely to be either chemisorbed atomic oxygen or the PtO-like surface oxide.

AUTHOR INFORMATION

Corresponding Author

sarpkaya@slac.stanford.edu

Notes

The authors declare no competing financial interest.

■ ACKNOWLEDGMENTS

This work was supported by the U.S. Department of Energy (DOE), Basic Energy Science (BES) under contract DE-AC02-76SF00515 through the SUNCAT Center for Interface Science and Catalysis and the Stanford Synchrotron Radiation Laboratory, a national user facility operated by Stanford University on behalf of the DOE, Office of BES. The ALS and the MES beamline 11.0.2 are supported by the Director, Office of Science, Office of Basic Energy Sciences, Division of Chemical Sciences, Geosciences, and Biosciences and Materials Sciences Division of the US Department of Energy at the Lawrence Berkeley National Laboratory under contract no. DE-AC02-05CH11231.

■ REFERENCES

(1) Völkening, S.; Wintterlin, J. *J. Chem. Phys.* **2001**, *114*, 6382−6395.
(2) Wintterlin, J.; Völkening, S.; Janssens, T. V. W.; Zambelli, T.; Ertl, G. *Science* **1997**, *278*, 1931−1934.
(3) Weaver, J. F.; Chen, J.-J.; Gerrard, A. L. *Surf. Sci.* **2005**, *592*, 83−103.
(4) Su, X.; Cremer, P. S.; Shen, Y. R.; Somorjai, G. A. *J. Am. Chem. Soc.* **1997**, *119*, 3994−4000.
(5) Somorjai, G. A. *Introduction to surface chemistry and catalysis*; 2nd ed.; Wiley: Hoboken, N.J., 2010.
(6) Kinne, M.; Fuhrmann, T.; Zhu, J. F.; Whelan, C. M.; Denecke, R.; Steinrück, H.-P. *J. Chem. Phys.* **2004**, *120*, 7113−7122.
(7) Ackermann, M. D.; Pedersen, T. M.; Hendriksen, B. L. M.; Robach, O.; Bobaru, S. C.; Popa, I.; Quiros, C.; Kim, H.; Hammer, B.; Ferrer, S.; Frenken, J. W. M. *Phys. Rev. Lett.* **2005**, *95*, 255505.
(8) Hendriksen, B. L. M.; Frenken, J. W. M. *Phys. Rev. Lett.* **2002**, *89*, 046101.
(9) Gao, F.; Wang, Y.; Cai, Y.; Goodman, D. W. *J. Phys. Chem. C* **2009**, *113*, 174−181.
(10) Van Rijn, R.; Balmes, O.; Felici, R.; Gustafson, J.; Wermeille, D.; Westerström, R.; Lundgren, E.; Frenken, J. W. M. *J. Phys. Chem. C* **2010**, *114*, 6875−6876.
(11) Gerrard, A. L.; Weaver, J. F. *J. Chem. Phys.* **2005**, *123*, 224703−224703−17.
(12) Alayon, E. M. C.; Singh, J.; Nachtegaal, M.; Harfouche, M.; van Bokhoven, J. A. *J. Catal.* **2009**, *263*, 228−238.
(13) Weaver, J. F. *Chem. Rev.* **2013**, *113*, 4164−4215.
(14) Wang, J. G.; Li, W. X.; Borg, M.; Gustafson, J.; Mikkelsen, A.; Pedersen, T. M.; Lundgren, E.; Weissenrieder, J.; Klikovits, J.; Schmid, M.; Hammer, B.; Andersen, J. N. *Phys. Rev. Lett.* **2005**, *95*, 256102.
(15) Butcher, D. R.; Grass, M. E.; Zeng, Z.; Aksoy, F.; Bluhm, H.; Li, W.-X.; Mun, B. S.; Somorjai, G. A.; Liu, Z. *J. Am. Chem. Soc.* **2011**, *133*, 20319−20325.
(16) Li, W. X. *J. Phys.: Condens. Matter* **2008**, *20*, 184022.
(17) Miller, D. J.; Öberg, H.; Kaya, S.; Sanchez Casalongue, H.; Friebel, D.; Anniyev, T.; Ogasawara, H.; Bluhm, H.; Pettersson, L. G. M.; Nilsson, A. *Phys. Rev. Lett.* **2011**, *107*, 195502.
(18) Li, W. X.; Österlund, L.; Vestergaard, E. K.; Vang, R. T.; Matthiesen, J.; Pedersen, T. M.; Lægsgaard, E.; Hammer, B.; Besenbacher, F. *Phys. Rev. Lett.* **2004**, *93*, 146104.
(19) Ogletree, D. F.; Bluhm, H.; Lebedev, G.; Fadley, C. S.; Hussain, Z.; Salmeron, M. *Rev. Sci. Instrum.* **2002**, *73*, 3872−3877.
(20) Björneholm, O.; Nilsson, A.; Tillborg, H.; Bennich, P.; Sandell, A.; Hernnäs, B.; Puglia, C.; Mårtensson, N. *Surf. Sci.* **1994**, *315*, L983−L989.
(21) Puglia, C.; Nilsson, A.; Hernnäs, B.; Karis, O.; Bennich, P.; Mårtensson, N. *Surf. Sci.* **1995**, *342*, 119−133.
(22) Steininger, H.; Lehwald, S.; Ibach, H. *Surf. Sci.* **1982**, *123*, 1−17.
(23) Pedersen, T. M.; Li, W. X.; Hammer, B. *Phys. Chem. Chem. Phys.* **2006**, *8*, 1566−1574.
(24) Li, W. X.; Hammer, B. *Chem. Phys. Lett.* **2005**, *409*, 1−7.
(25) Reutt-Robey, J. E.; Doren, D. J.; Chabal, Y. J.; Christman, S. B. *J. Chem. Phys.* **1990**, *93*, 9113−9129.
(26) Ellinger, C.; Stierle, A.; Robinson, I. K.; Nefedov, A.; Dosch, H. *J. Phys.: Condens. Matter* **2008**, *20*, 184013.
(27) Farkas, A.; Zalewska-Wierzbicka, K.; Bachmann, C.; Goritzka, J.; Langsdorf, D.; Balmes, O.; Janek, J.; Over, H. *J. Phys. Chem. C* **2013**, *117*, 9932−9942.
(28) Chen, M. S.; Cai, Y.; Yan, Z.; Gath, K. K.; Axnanda, S.; Goodman, D. W. *Surf. Sci.* **2007**, *601*, 5326−5331.